Shell mineralogy of a foundational marine species, *Mytilus californianus*, over half a century in a changing ocean

Elizabeth M. Bullard[a,1], Ivan Torres[b], Tianqi Ren[b], Olivia A. Graeve[b], and Kaustuv Roy[a]

[a]Section of Ecology, Behavior and Evolution, University of California San Diego, La Jolla, CA 92093-0116; and [b]Department of Mechanical and Aerospace Engineering, University of California San Diego, La Jolla, CA 92093-0411

Edited by Jeremy B.C. Jackson, American Museum of Natural History, New York, NY, and approved November 10, 2020 (received for review March 13, 2020)

Anthropogenic warming and ocean acidification are predicted to negatively affect marine calcifiers. While negative effects of these stressors on physiology and shell calcification have been documented in many species, their effects on shell mineralogical composition remains poorly known, especially over longer time periods. Here, we quantify changes in the shell mineralogy of a foundation species, *Mytilus californianus*, under 60 y of ocean warming and acidification. Using historical data as a baseline and a resampling of present-day populations, we document a substantial increase in shell calcite and decrease in aragonite. These results indicate that ocean pH and saturation state, not temperature or salinity, play a strong role in mediating the shell mineralogy of this species and reveal long-term changes in this trait under ocean acidification.

ocean acidification | foundational marine species | mineralogy

There is increasing concern about the effects of anthropogenic stressors, particularly warming and ocean acidification (OA), on marine calcifiers (organisms that precipitate a calcium carbonate ($CaCO_3$) exoskeleton). Short-term experimental studies, spanning days to months (1, 2), have shown negative impacts of OA on the physiology of calcifiers (3), inhibition of shell and soft body growth (3), and decreased functionality of the shell (4). Some experiments also suggest that rising temperatures can synergistically augment the effects of OA (5), while others show no impact on shell calcification (2) or even an increase in calcification rate with increasing temperature (6). Although an increasing number of experimental studies are investigating the biological effects of OA and warming, very little information is available on the long-term responses of calcification for wild populations of marine calcifiers to these stressors. Additionally, the few studies available that assess changes in calcification in response to warming and OA on decadal to centennial time scales show contrasting results. For example, comparison of specimens of the intertidal mussel, *Mytilus californianus*, from archeological middens (~1000 to 2420 y BP) with those from living populations showed a significant thinning of the shell (7) and loss of mineralogical control (8). In contrast, an analysis of shell thickness over a 120-y period in a brachiopod (*Calloria inconspicua*) from New Zealand showed no change in thickness through time (9). Furthermore, effects of anthropogenic stressors on the mineralogical composition of the shell, a key functional trait, still remain poorly quantified on both short and long time scales (but see ref. 4 for a short-term assessment). Here, we use historical measurements in conjunction with field sampling to quantify the impact of half a century of ocean warming and OA on the shell mineralogy of multiple populations of *M. californianus*, a foundational marine bivalve species along the northeastern Pacific coast.

The shells of marine mollusks are composed of two different polymorphs of $CaCO_3$, namely aragonite and calcite (10). Of these two polymorphs, aragonite is more soluble than calcite (11), though differences in crystal size and organic content of the shell can also play a role in mediating dissolution rates of mollusk shells (12–14). While most molluscan species tend to have shells that are predominantly made of either aragonite or calcite, others have shells that contain both polymorphs. It has long been hypothesized that the ratio of aragonite to calcite (in this study represented as the percentage of aragonite) in the shells of species with mixed mineralogy is mediated by the temperature and/or $CaCO_3$ saturation state of seawater (13, 15). This is supported by the observation that aragonite content of molluscan shells in species with mixed mineralogy changes predictably along a latitudinal gradient, with an enrichment of aragonite as compared to calcite in warmer waters (13, 15). Furthermore, larvae of a marine mussel with mixed mineralogy (*M. edulis*) grown under high partial pressure of carbon dioxide (pCO_2) conditions were enriched in calcite compared to those grown under lower pCO_2 conditions (16). Given that aragonite is preferentially precipitated in warmer waters compared to calcite in species with mixed mineralogy, anthropogenic warming by itself should favor higher aragonite content in shells of species that use both polymorphs, while the decrease in carbonate ions and saturation state of $CaCO_3$, primarily aragonite, in conjunction with increasing pCO_2 and decreasing ocean pH should favor calcite.

Along the northeastern Pacific coast, sea surface temperatures (SSTs) have increased significantly since the 1950s (*SI Appendix*, Table S1). Over this time, anthropogenic CO_2 emissions have also increased substantially (17, 18), leading to decreases in ocean pH and saturation state (18), although the exact magnitude of such

Significance

Anthropogenic ocean acidification (OA) is a potential threat for marine calcifying organisms. While much experimental work has been done to assess the impacts of OA on marine calcifiers, studies over long temporal scales and across multiple populations still remain limited. Here, we combine historical data with recent field surveys to quantify the plasticity in shell mineralogy, a key functional trait, of a foundational marine bivalve, *Mytilus californianus*. Our data suggest that mineralogy in this species is responding more to pH and saturation state changes than warming or decreasing salinity. This study highlights the importance of utilizing long-term data sets and large spatial comparisons to understand and test predictions about species responses to a changing world.

Author contributions: E.M.B. and K.R. designed research; E.M.B. and I.T. performed research; O.A.G. contributed new reagents/analytic tools; E.M.B., T.R., O.A.G., and K.R. analyzed data; and E.M.B., I.T., T.R., O.A.G., and K.R. wrote the paper.

The authors declare no competing interest.

This article is a PNAS Direct Submission.

[1]To whom correspondence may be addressed. Email: embullar@ucsd.edu.

This article contains supporting information online at https://www.pnas.org/lookup/suppl/doi:10.1073/pnas.2004769118/-/DCSupplemental.

published January 11, 2021.

decreases along the northeastern Pacific remains unknown. We quantified how the aragonite content of shells of *M. californianus* populations have changed in response to these opposing forces by comparing baseline measurements of aragonite content of shells collected in 1952 [hereafter referred to as sample S52 (10)] and 1958 to 1960 [sample S58-60 (19)] with those from samples collected in 2017 and 2018 (sample S17-18) (*SI Appendix*, Table S2). Specifically, we sampled five populations of *M. californianus* along a spatial gradient spanning 15° of latitude along the northeastern Pacific coast (Fig. 1), a transect similar to that from the late 1950s (19). Three of our sites in Southern California are the same as those from the late 1950s (19), and one matched site, La Jolla, additionally has data from 1952 (S52) (10); the other two sites further north are in the same regions sampled in the late 1950s study (19) but are not exact matches (Fig. 1 and *SI Appendix*, Fig. S1). Although the northern sites are not exact spatial matches with our baseline data, by sampling the same regions as in the 1950s (19), they allow us to investigate whether the latitudinal gradient in shell aragonite content of this species has changed over time. For two of our matched sites (La Jolla and Corona Del Mar), samples from 2010 (hereafter S10) were also available, providing an additional baseline that further allows us to assess decadal responses of shell mineralogy to warming and ocean acidification. For all of the comparisons, individuals of *M. californianus* sampled live in 2017-2018 (S17-18) were matched to the same body-size range as in the baseline studies to avoid any impact of size on shell aragonite content, and all samples were prepared following the same procedures described in the baseline studies (10, 19) and analyzed using X-ray diffraction (XRD) (see *Materials and Methods*).

Results and Discussion

At all three of our matched sites, large temporal changes in shell aragonite content are evident. At La Jolla, the shell aragonite content decreased significantly from the 1950s (S58-60) to 2010 (S10) and has been stable since (Fig. 1 and *SI Appendix*, Fig. S1 and Tables S3 and S4). Avila Beach shows a similar trend with a significant decrease in aragonite content from the 1950s (S58-60) to 2017-2018 (S17-18) (Fig. 1 and *SI Appendix*, Fig. S1 and Tables S3 and S4). At Corona del Mar, the trend is more complex, with a significant decline in aragonite content from the 1950s to 2010, but with subsequent recovery, so that the aragonite content of S17-18 is not significantly different from that of S58-60 (Fig. 1 and *SI Appendix*, Fig. S1 and Table S3).

Further north at Crescent City, only one sample from 1959 (S59) is available, making statistical comparisons impossible, but qualitative assessment is still feasible and informative. At this site, there has been an increase in temperature through time (*SI Appendix*, Tables S1 and S5) and a corresponding change in shell aragonite content, from 42.90% aragonite in sample S59 to a median value of 16.82% and a maximum of 23.38% in sample S17-18 (*SI Appendix*, Table S6). Thus, the 42.90% measured in 1959 is well outside the current range of our data despite a substantially larger sample (n = 9; *SI Appendix*, Tables S2 and S6).

The temporal decrease in shell aragonite content seen at each of our matched sites is also evident over a wider latitudinal gradient (Fig. 1*E* and *SI Appendix*, Fig. S1*E*). Regression models that take in to account spatial and temporal autocorrelations as well as potential effects of shell size and weight (lagged-mixed simultaneous autoregressive models, generalized least squares models, and linear mixed effect models with locality added as a random effect; see *Materials and Methods*) all show a significant difference in the latitudinal trends in shell aragonite content between the late 1950s and 2017-2018 (Fig. 1*E* and *SI Appendix*, Table S4). Specifically, there was a significant latitudinal trend in shell aragonite content during the 1950s, with higher latitudes being preferentially enriched in calcite (*SI Appendix*, Table S4). In contrast, latitude is not a significant predictor of aragonite content in 2017-2018 (*SI Appendix*, Table S4), suggesting an overall shallowing of the slope of this relationship through time, driven by larger decreases in shell aragonite content at our southern sites compared to northern ones. Overall, shell aragonite content has decreased substantially across the range of this species. The difference in percentage of aragonite is more pronounced if S52 and S10 data are added to the analyses with the slopes becoming significantly different between the past (S52 and S58-60) and recent times (S10 and S17-18) (*SI Appendix*, Table S3 and Fig. S1). Because temperature varies substantially with latitude, we also assessed changes in the relationship between shell aragonite

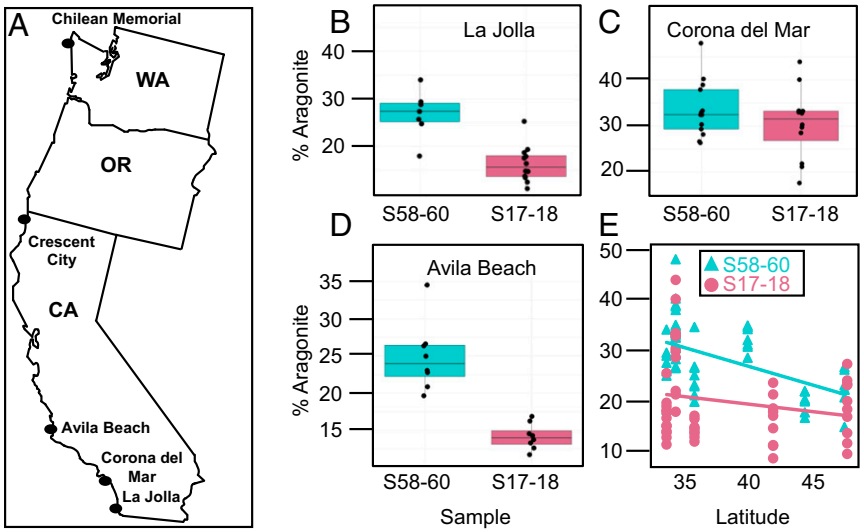

Fig. 1. (*A*) Locality map showing the five sites for samples S17-18. Three of the sites, Avila Beach (n = 8 for both S58-60 and S17-18), Corona del Mar (n = 14 for S58-60 and n = 12 for S17-18), and La Jolla (n = 7 for S58-60 and n = 12 for S17-18), in California, are the same as those in the late 1950's. The other two, Crescent City, California, and Chilean Memorial, Washington, are in the same region as northern sites sampled in 1958-1960 (see main text, *Materials and Methods*). The box plots show comparisons of the percentage of aragonite for S58-60 and S17-18. The samples S17-18 are significantly more enriched in calcite compared to those from the past (*SI Appendix*, Table S3). (*B*) La Jolla comparison. (*C*) Corona del Mar comparison. (*D*) Avila Beach comparison. (*E*) Relationship between percentage of aragonite in individual *M. californianus* shells and latitude for S58-60 (n = 50) and S17-18 (n = 51). The slopes are not significantly different between the two time periods (*SI Appendix*, Table S3).

content and SST (*SI Appendix*, Fig. S2). Similar to the difference in latitudinal trends, temperature is a significant predicter of percentage of aragonite in our most conservative spatial autocorrelation models controlling for size and weight for the late 1950s, but this relationship is not significant for our 2017-2018 samples (*SI Appendix*, Table S4 and Fig. S3).

In addition to SST and pH, an inverse relationship between salinity and shell aragonite content in Eastern Pacific mussels (*M. californianus* and *Mytilus galloprovincialis*) has also been hypothesized (10, 15). This is in contrast to recent observations of *M. edulis* and *Mytilus trossolus* in the Baltic, where a decrease in aragonite content was evident with decreasing salinity (13). This potential difference in salinity response provides an interesting comparative framework for looking at how species with different evolutionary histories and different environmental regimes respond to the same stressor. In this case, *M. californianus* has evolved in a very different oceanographic regime (i.e., upwelling system) compared to *M. edulis*, the focus of the Baltic study. Furthermore, changes in salinity have also been shown to affect the metabolic cost of shell calcification (20), highlighting the importance of understanding how salinity changes affect shell mineralogy of species with different evolutionary and environmental histories. At all three of our southern matched sites, both SST and salinity has changed since the 1950s. SST has increased from the 1950s to 2017-2018, but the magnitude of this change varies across sites, with the largest temporal change in our warmest site, La Jolla (*SI Appendix*, Table S1). Over this time, salinity has decreased at each of our sites but, again, by different magnitudes (*SI Appendix*, Tables S1 and S5). Although the temporal data on temperature and salinity are too sparse for quantitative analyses at the level of individual sites given there are just two time points for Avila Beach and three for Corona del Mar and La Jolla, qualitatively, the directionality of the observed trends do not support the predicted relationships between temperature, salinity, and shell aragonite content for Eastern Pacific *Mytilus* species at any of the three sites analyzed here.

Overall, our results indicate that the aragonite content of *M. californianus* shells has declined significantly over the last half century. While the magnitude of this decrease varies across our sites, it is clear that most populations of this species incorporate much more calcite in their shells now than in the past. Our results also show that these decreases are not due to temperature or salinity change. Other factors such as predation pressure, wave exposure, and food availability are also known to affect shell calcification (7, 21), but whether they have any influence on shell mineralogy remains unclear. In fact, selection due to increased predation pressure and/or wave exposure should lead to an increase in shell aragonite content since it is the stronger of the two polymorphs (10). Age and growth rates of individuals can potentially also affect the proportion of aragonite/calcite within the shell. Individuals of *M. californianus* are extremely difficult to age from shell growth lines (10, 22), so we cannot rule out the possibility of some age-related effects, such as decreased longevity or changing growth rates, in our data. However, size and age are tightly and positively correlated in this species (19), and the lack of any significant size effects in our regression models suggest that temporal differences in age are unlikely to be a major driver of our results. One aspect of anthropogenic change that affects both shell calcification and mineralogy is changes in sea water saturation state and ocean pH (4, 16). Long-term measurements of these variables are not available at any of our sites, making it impossible to directly test the role of OA in driving the temporal changes seen here. However, multiple indirect lines of evidence suggest a major role of OA. For example, short-term experiments have shown a decrease in shell aragonite content in *M. edulis* larvae of parents grown under higher pCO_2 conditions (1,000 microatmospheres, or μatm) compared to offspring of parents grown under lower pCO_2 conditions (380, 550, and 750 μatm) (16). Similarly, the eastern oyster, *Crassostrea virginica*, shows an increase in the calcite laths within the shells of juveniles grown under treatments of 3,500 μatm as compared to those grown under 380 μatm, suggesting in both cases a response to elevated pCO_2 and decreased pH (23). On a larger spatial scale, the Atlantic mussels *M. edulis* and *M. trossolus* show an increase in the thickness of the calcitic prismatic layer in the shell from temperate to polar regions (13). Finally, long-term changes in the crystallographic structure of the shell of *M. californianus* has also been attributed to changing ocean pH (8). Thus, our results are consistent with experimental evidence of preferential precipitation of the less soluble calcite over aragonite under OA. While preferential dissolution of precipitated aragonite in response to more corrosive waters (21) can also affect the calcite/aragonite ratio of shells, we did not see any clear signs of dissolution such as substantial pitting of the shells in samples S10 and S17-18, and since those shells do not weigh significantly less than those from the 1950s (S58-60), it is likely that differential precipitation of calcite, rather than dissolution of aragonite due to OA, is the primary driver of our results.

Regardless of the exact cause(s) of the change in minerology of *M. californianus,* our results clearly demonstrate that shells of this species, across most of its geographic range, have significantly more calcite today compared to the 1950s. This suggests that marine calcifiers with mixed mineralogy may have considerable plasticity to adjust the ratio of different polymorphs of $CaCO_3$ in their shells in response to global change. While such plasticity may be advantageous in future ocean environments, as pH is expected to drop even more and higher latitudes are predicted to be undersaturated with respect to aragonite by the end of this century (24), there may also be functional trade-offs in decreasing shell aragonite content. For example, *M. edulis* larvae precipitating only calcite when born from parents raised in the highest pCO_2 treatment tend to show loss of crystallographic control (4). Calcite precipitated under these higher pCO_2 conditions (1,000 μatm) may also be more brittle (4), potentially making shells more prone to fracturing under durophagous predation. Further investigation of such functional trade-offs is needed to better predict the potential for adaptation of *M. californianus*, a foundation species, and other marine calcifiers with mixed mineralogy to future OA. Finally, the work presented here highlights the importance of long-term comparisons to better understand the responses of marine calcifiers to anthropogenic global change. Such comparisons not only document how wild populations are responding to changing conditions but also help test predictions derived from short-term experiments.

Materials and Methods

Collecting Localities and Historical Data. We extracted historical information about collecting locality, environmental variables, morphometric measurements, and shell mineralogical compositions of *M. californianus* along the northeastern Pacific from two primary sources, namely Lowenstam (10) (S52) and Dodd (19) (S58-60) (*SI Appendix*, Table S5). From ref. 10, we only used data for live-collected individuals from La Jolla, California, collected on December 26, 1952, and within the same size range as the samples collected by Dodd (19). The exact location of where samples were collected by Lowenstam (10) is unknown but is most likely from around the Scripps Institution of Oceanography (SIO) campus, where we collected our live samples. Dodd (19) collected his samples between 1958 and 1960 (S58-60) from six localities (19) but provided a specific date of collection (month/day) only for the Corona del Mar site. This site is also the only locality accompanied by a detailed explanation of sample collection. The other sampling sites in ref. 19 are described as locality names without information about their latitude and longitude. However, we were able to confirm that the La Jolla, California, samples were collected from the pier pilings at SIO. The Avila Beach, California, samples were also very likely to have been collected from the pier pilings there. The name associated with the northern (Washington) locality in ref. 19 is somewhat ambiguous (see below). Thus, we directly matched

ECOLOGY

three of the sites from ref. 19, while for Washington, we sampled the same region as Dodd.

To compare mineralogical changes (specifically shell aragonite content) through time, we collected *M. californianus* in 2017 and 2018 (S17-18) at the three sites that we were able to match from ref. 19, La Jolla (32.8663°N, 117.2546°W), Corona del Mar (33.5979°N, 117.8730°W), and Avila Beach (35.1800°N, 120.7319°W) in California. Additionally, we collected from two other sites, the Battery Point Lighthouse in Crescent City, California (41.7441°N, 124.2031°W), and Chilean Memorial, Washington (47.9643°N, 124.6635°W), to construct a latitudinal gradient comparable to that from ref. 19 (Fig. 1*A*). Crescent City is actually a site included in ref. 19, but the exact location of the collection within this city is unknown, and only data for one individual is included in ref. 19. Therefore, this site is a partial match where statistical analyses of temporal trends are not possible; only qualitative comparisons are provided here. Dodd's (19) northernmost site ("Hoh, Washington") could potentially refer to three different locations, so we chose Chilean Memorial, a site in the same region, as our northernmost site. More detailed information on each site can be found in *SI Appendix*.

At each locality, we collected individuals of *M. californianus* within the same size range as those from ref. 19 (*SI Appendix*, Table S6) from wave-exposed sites in the middle portion of the mussel zone. Exact replication of each individual's size was only possible at Avila Beach, where the populations were plentiful and a myriad of size classes existed at time of collection. Exactly matching the entire size range was not feasible at other sites, such as Corona del Mar, primarily because the largest individuals (>100 mm) are no longer present intertidally at these locations, most likely due to human harvesting [e.g., (25)]. To address this problem, we excluded any individuals from samples S58-60 that were too large to be found intertidally today. While age of individuals can also potentially affect the aragonite/calcite ratios of their shells, we focus on size (i.e., length) and weight (as a proxy for thickness) in our analyses here for multiple reasons: 1) information about the age of the specimens from the 1950s is not available, but sizes of those specimens are known; 2) qualitative aging of *M. californianus* is difficult if not impossible at many locations where we sampled this species [e.g., (22)], but in localities where aging is possible, a positive relationship between size and age has been documented for *M. californianus* (19, 26, 27); 3) recent analyses of shell calcification have largely used specimen size as a proxy for age (13, 28).

In addition to 2017-2018 (S17-18) samples, we also used samples collected in 2010 (S10) at two of the matched sites, La Jolla and Corona del Mar. These samples were also size matched to sanples S58-60 with a similar cutoff for the largest individuals, as explained above.

We used the environmental data from refs. 10 and 19 for our comparison, though ref. 10 only contains temperature data. In addition, ref. 19 explicitly states that temperature data listed in the study is a 10-y average, but whether such averaging also applies to ref. 10 is unclear. Since the majority of our data came from ref. 19, we chose to use the 10-y mean annual temperature collected from the nearest buoy station (29, 30) for 2017-2018 (*SI Appendix*, Table S1). For 2010 at Corona del Mar, a 5-y average was used because data did not cover the whole 10-y average range (29). The late 1950s data from ref. 19 only records salinity "at time of collection," so we used the average salinity measurement for the day of collection for our 2010 and 2017-2018 samples (29, 30).

Shell Mineralogy Quantification Using XRD. We followed the methods stated in ref. 19 to quantify the shell mineralogical compositions of our samples so that our values are directly comparable to those from the 1950s studies. Note that the methods described in Dodd's Ph.D. thesis (19) also apply to ref. 10, since the work was completed under Lowenstam's supervision. The percentage of aragonite data in ref. 19 represents a mixture of single valve, whole individual, and multiple individuals. For this study, we only use the data from ref. 19 that are from single valves and use the relevant analytical method. Briefly, we first cleaned the shells of *M. californianus* of epibionts. We then placed a single valve from each individual in commercial Chlorox bleach with a concentration of 5.25% sodium hypochlorite for 3 to 7 d to remove the periostracum as described in refs. 19 and 10. We then rinsed the valve with deionized water and dried it in a fume hood at ambient temperature until the weight of the valve did not change from water loss. Once dry, we ground each valve in its entirety by hand in an agate mortar and pestle until a grain size of less than No. 200 (75 μm) mesh was achieved (19). To avoid any possible conversion of aragonite to calcite, we first broke the shell into pieces and slowly ground them in small batches with continuous removal of the finer grains passing through the No. 200 mesh sieve (75 μm) (10, 19).

The powder for each individual valve was analyzed using a D2 Phaser X-ray diffractometer (Bruker AXS, Madison, WI). For each individual sample, the resulting powder was divided into three parts in order to run independent measurements, which were then averaged. The procedure consisted of passing the powdered samples through a No. 100 mesh (150 μm) sieve onto a silicon crystal zero-background disk, as described by ref. 19. The surface of the zero-background disk was covered in a thin layer of petroleum jelly, which allowed the fragments to randomly adhere upon the platform and minimize any effect of preferred orientation (19). Prior to any subsequent runs, the sieve was rinsed with water and fully dried, and the silicon disk was cleaned with ethanol in order to ensure each sample was unaffected by previous runs. The XRD runs were carried out using copper K-alpha (CuKα) radiation with a step size of 0.01° 2θ ranging from 20° to 60°, with each sample run lasting ∼37 min. We used *Littorina keenae* collected from the rocky intertidal area near SIO and commercially raised *Crassostrea gigas* as our pure biogenic aragonite and calcite standards, respectively. XRD patterns for both *L. keenae* and *C. gigas* were obtained to confirm their purity. We ground the *L. keenae* and *C. gigas* standards to the same grain size as the test samples (i.e., <75 μm) and followed the procedure above to create a calibration curve. We analyzed the diffraction peaks using TOPAS 4.2 software (DIFFRAC^{Topas}, Bruker AXS) and determined percentage of aragonite by means of Rietveld refinement. This methodology allows refinement through a least-squares algorithm by evaluating user-defined parameters that minimize the difference between an experimental pattern and a model based on crystal structure and instrumental parameters. These latter parameters help constrain peak positions and peak intensities, respectively (31). In accordance with this technique, each raw diffraction pattern per individual run was loaded into TOPAS and compared with the calibration curve and standard calcite and aragonite values. These values were made accessible via the Inorganic Crystal Structure Database (ICSD) (32, 33). With respect to the instrumental parameters, a CuKα emission profile was loaded, along with a fourth-order Chebychev polynomial background function to filter the data. The goniometer radii of our specific system were set to 141 mm, while the zero-error correction was utilized in order to account for any peak shifts that could arise due to systematic error. This correction ensures all peaks are shifted by a constant value, independent of θ angle (34). Calcite and aragonite structures were added accordingly, with the respective lattice parameters taken via ICSD, along with the atomic sites necessary for each structure. During the process, it is also safe to assume that there is no preferred orientation, that is, the orientation of the crystallites is considered to be random. This random orientation otherwise indicates that all possible orientations of crystallites within the sample occur with the same probability (34). All parameters (i.e., overall intensities, background, peak positions, peak shapes, and structures) were set to be refined during the calculation. The Rietveld refinement was then run for three iterations to obtain consistent R values as the phase composition is carried out. The resulting values are a final phase ratio indicating the amount of calcite and aragonite within each individual measurement as a percentage.

Statistical Analyses. We first tested for a significant difference in percentage of aragonite between left and right valves at each of our 2017-2018 (S17-18) localities using Wilcoxon rank sum tests. Since there was no significant difference (*SI Appendix*, Fig. S4 and Table S3), we did not differentiate data from left and right valves for subsequent analyses.

We used Kruskal–Wallis rank sum tests to determine if percentage of aragonite had significantly changed at our three matched sites through time. Kruskal–Wallis was used instead of a Student's *t* test because percentage of aragonite is a ratio, and assessing statistical changes in the median is more informative than the mean in such cases. Additionally, we conducted F-tests to determine significant changes in variation for matched sites through time.

We tested for temporal and spatial autocorrelation using the Durbin–Watson test (35) and Moran's I (36), respectively. Durbin–Watson tests were run using the lmtest package in R (37) and Moran's I using the Ape package (38). Data were temporally and spatially autocorrelated (*SI Appendix*, Table S3), so we ran multiple models to account for such autocorrelation and selected the best model using Akaike information criterion (AIC) scores. To account for temporal autocorrelation, we used the Cochrane–Orcutt method (39) using the Orcutt package in R (40). The base of the model was a linear regression model comparing percentage of aragonite as a function of time, latitude, temperature, length, and weight (*SI Appendix*, Table S4). We used the temperature data associated with S58 -60 (19) and S17-18 (29, 30) for our main comparison. In addition, we compared all past data (S52 (10) and S58-60 (19) combined) with all recent samples [S10 (29, 30) and S17-18 (29, 30) combined] for our full analyses. To control for spatial autocorrelation, we

ran three different types of models, each of which evaluated percentage of aragonite as a function of latitude and temperature as well as length and weight to account for potential size effects on the mineralogical composition. The three different models we tested were 1) generalized least square models, 2) linear mixed effect models (LME) with locality as a random effect, and 3) simultaneous autoregressive models with a mixed lagged effect and locality as a random effect to account for spatial autocorrelation in multiple directions using the spatialreg package in R (41). All models used restricted maximum likelihood. Regardless of which model we used, the results were qualitatively the same. However, model comparison using AIC suggested that the best-performing model was an LME with locality as a random effect. We thus used LME with locality as a random effect to test for differences in slopes between samples S58-60 and S17-18, as well as the slope between combined past (S52 and S58-60) and combined recent (S10 and S17-18). To further control for any potential nonlinear effect of size on our latitudinal or temperature trends, we used the residuals from a linear regression of percentage of aragonite and length against latitude and temperature (*SI Appendix*, Fig. S5 and Table S4). All analyses were carried out in R (42).

Data Availability. All study data are included in the article and *SI Appendix*.

ACKNOWLEDGMENTS. We thank A. Neu for aiding in sample collection and helpful discussions about this work. This work was partially supported by a grant from the NASA (to K.R.) and the Jeanne Marie Messier Memorial Endowment Fund (to E.M.B.).

1. K. J. Kroeker *et al*., Impacts of ocean acidification on marine organisms: Quantifying sensitivities and interaction with warming. *Glob. Change Biol.* **19**, 1884–1896 (2013).
2. E. L. Cross, E. M. Harper, L. S. Peck, Thicker shells compensate extensive dissolution in brachiopods under future ocean acidification. *Environ. Sci. Technol.* **53**, 5016–5026 (2019).
3. K. J. Kroeker, R. L. Kordas, R. N. Crim, G. G. Singh, Meta-analysis reveals negative yet variable effects of ocean acidification on marine organisms. *Ecol. Lett.* **13**, 1419–1434 (2010).
4. S. C. Fitzer *et al*., Ocean acidification alters the material properties of *Mytilus edulis* shells. *J. R. Soc. Interface* **12**, 1–8 (2015).
5. H. S. Findlay, M. A. Kendall, J. I. Spicer, S. Widdicombe, Relative influences of ocean acidification and temperature on intertidal barnacle post-larvae at the northern edge of their geographic distribution. *Estuar. Coast. Shelf Sci.* **86**, 675–682 (2010).
6. G. G. Waldbusser, E. P. Voigt, H. Bergshneider, M. A. Green, R. I. E. Newell, Biocalcification in the eastern oyster (*Crassostrea virginica*) in relation to long-term trends in the Chesapeake Bay pH. *Estuaries Coasts* **34**, 221–231 (2011).
7. C. A. Pfister *et al*., Historical baselines and the future of shell calcification for a foundation species in a changing ocean. *Proc. Biol. Sci.* **283**, 1–8 (2016).
8. S. J. McCoy, N. A. Kamenos, P. Chung, T. J. Wootton, C. A. Pfister, A mineralogical record of ocean change: Decadal and centennial patterns in the California mussel. *Glob. Change Biol.* **24**, 2554–2562 (2018).
9. E. L. Cross, E. M. Harper, L. S. Peck, A 120-year record of resilience to environmental change in brachiopods. *Glob. Change Biol.* **24**, 2262–2271 (2018).
10. H. A. Lowenstam, Factors affecting the aragonite: Calcite ratios in carbonate-secreting marine organisms. *J. Geol.* **62**, 284–322 (1954).
11. J. D. Currey, J. D. Taylor, The mechanical behavior of some molluscan hard tissues. *J. Zool.* **173**, 395–406 (1974).
12. E. M. Harper, Are calcitic layers an effective adaptation against shell dissolution in the Bivalvia? *J. Zool. (Lond.)* **251**, 179–186 (2000).
13. L. Telesca *et al*., Biomineralization plasticity and environmental heterogeneity predict geographic resilience patterns of foundation species to future change. *Glob. Change Biol.* **25**, 1–15 (2019).
14. M. Chadwick, E. M. Harper, A. Lemasson, J. I. Spicer, L. S. Peck, Quantifying susceptibility of marine invertebrate biocomposites to dissolution in reduced pH. *R. Soc. Open Sci.* **6**, 190252 (2019).
15. J. R. Dodd, Paleoecological implications of shell mineralogy in two pelecypod species. *J. Geol.* **71**, 1–11 (1963).
16. S. C. Fitzer, M. Cusack, V. R. Phoenix, N. A. Kamenos, Ocean acidification reduces the crystallographic control in juvenile mussel shells. *J. Struct. Biol.* **188**, 39–45 (2014).
17. H. A. Keeling *et al*., "Atmospheric CO2 and 13CO2 exchange with the terrestrial biosphere and oceans from 1978 to 2000: Observations and carbon cycle implications" in *A History of Atmospheric CO2 and Its Effects on Plants, Animals, and Ecosystems*, M. D. Ehleringer, J. R. Cerling, T. E. Dearing, Eds. (Springer Verlag, 2005), pp. 83–113.
18. R. A. Feely, S. C. Doney, S. R. Cooly, Ocean acidification – present conditions and future changes. *Oceanography (Wash. D.C.)* **22**, 36–47 (2009).
19. J. R. Dodd, *Paleoecological Implications of the Mineralogy, Structure, and Strontium and Magnesium Contents of Shells of the West Coast Species of the Genus Mytilus* (California Institute of Technology, Pasadena, CA, 1961).
20. T. Sanders, L. Schmittmann, J. C. Nascimento-Schulze, F. Melzner, High calcification costs limit mussel growth at low salinity. *Front. Mar. Sci.* **5**, 1–9 (2018).
21. F. Melzner *et al*., Food supply and seawater pCO_2 impact calcification and internal shell dissolution in the blue mussel *Mytilus edulis*. *PLoS One* **6**, e24223 (2011).
22. T. H. Suchanek, The role of disturbance in the evolution of life history strategies in the intertidal mussels *Mytilus edulis* and *Mytilus californianus*. *Oecologia* **50**, 143–152 (1981).
23. E. Beniash, A. Ivanina, N. S. Lieb, I. Kurochkin, I. M. Sokolova, Elevated level of carbon dioxide affects metabolism and shell formation in oysters *Crassostrea virginica*. *Mar. Ecol. Prog. Ser.* **419**, 95–108 (2010).
24. S. Doney, W. Balch, V. Fabry, R. Feely, Ocean acidification: A critical emerging problem for the ocean sciences. *Oceanography (Wash. D.C.)* **22**, 16–25 (2009).
25. K. Roy, A. G. Collins, B. J. Becker, E. Begovic, J. M. Engle, Anthropogenic impacts and historical decline in body size of rocky intertidal gastropods in southern California. *Ecol. Lett.* **6**, 205–211 (2003).
26. C. A. Blanchette, B. Helmuth, S. D. Gaines, Spatial patterns of growth in the mussel, *Mytilus californianus*, across a major oceanographic and biogeographic boundary at Point Conception, California, USA. *J. Exp. Mar. Biol. Ecol.* **340**, 126–148 (2007).
27. H. L. Ford *et al*., Evaluating the skeletal chemistry of *Mytilus californianus* as a temperature proxy: Effects of microenvironment and ontogeny. *Paleoceanography* **25**, 1–14 (2010).
28. A. Piwoni-Piórewicz *et al*., Size effect on the mineralogy and chemistry of *Mytilus trossulus* shells from the southern Baltic Sea: Implications for environmental monitoring. *Environ. Monit. Assess.* **189**, 197 (2017).
29. Data from, "Southern California Coastal Ocean Observing System". https://ioos.noaa.gov/regions/sccoos/. Accessed 4 January 2019.
30. Center of Excellence in Marine Technology, Data from "National Oceanic and Atmospheric Administrations' national data buoy center". https://www.ndbc.noaa.gov/. Accessed 2 February 2019.
31. G. Will, *Powder Diffraction: The Rietveld Method and the Two Stage Method to Determine and Refine Crystal Structures from Powder Diffraction Data* (Springer, 2006).
32. E. N. Maslen, V. A. Streltsov, N. R. Streltsova, X-ray study of the electron density in calcite, $CaCO_3$. *Acta Crystallogr. B* **49**, 636–641 (1993).
33. T. Pilati, F. Demartin, C. M. Gramaccioli, Lattice-dynamical estimation of atomic displacement parameters in carbonates: Calcite and aragonite $CaCO_3$, dolomite $CaMg(CO_3)$ and magnesite $MgCO_3$. *Acta Crystallogr. B* **54**, 515–523 (1998).
34. H. W. King, E. A. Payzant, Error corrections for x-ray powder diffractometry. *Can. Metall. Q.* **40**, 385–394 (2001).
35. J. Durbin, G. S. Watson, Testing for serial correlation in least squares regression III. *Biometrika* **58**, 1–19 (1971).
36. C. F. Dormann *et al*., Methods to account for spatial autocorrelation in the analysis of species distributional data: A review. *Ecography* **30**, 609–628 (2007).
37. A. Zeilies, T. Hothorn, Diagnostic checking in regression relationships. *R. News* **2**, 7–10 (2002).
38. E. Paradis, K. Schliep, Ape 5.0: An environment for modern phylogenetics and evolutionary analyses in R. *Bioinformatics* **35**, 526–528 (2019).
39. W. D. Koenig, A. M. Liebhold, Temporally increasing spatial synchrony of North American temperature and bird populations. *Nat. Clim. Chang.* **6**, 614–617 (2016).
40. S. Stefano, M. Quartagno, M. Tamburini, D. Robinson, orcutt: Estimate procedure in case of first order autocorrelation (2018).
41. R. Bivand, G. Piras, Comparing implementations of estimation methods for spatial econometrics. *J. Stat. Softw.* **63**, 1–36 (2015).
42. R Core Team, R: A Language and Environment for Statistical Computing. R Foundation for statistical computing (2018).